

Strongly correlated electronic states and quasi-two-dimensional antiferromagnetism in honeycomb lattice compound $\text{In}_3\text{Cu}_2\text{VO}_9$

Da-Yong Liu¹, Ying Guo¹, Xiao-Li Zhang¹, Jiang-Long

Wang², Zhi Zeng¹, H. Q. Lin³ and Liang-Jian Zou^{1†*}

¹ *Key Laboratory of Materials Physics,*

Institute of Solid State Physics, Chinese Academy of Sciences,

P. O. Box 1129, Hefei, Anhui 230031, China

² *College of Physics Science and Technology,*

Hebei University, Baoding 071002, China

³ *Department of Physics, Chinese University of Hong Kong,*

Shatin, New Territory, Hong Kong, China

(Dated: November 5, 2018)

Abstract

We present electronic and magnetic properties of a honeycomb compound $\text{In}_3\text{Cu}_2\text{VO}_9$ in this paper. We find that undoped parent phase is a charge transfer insulator with an energy gap of 1.6 eV. Singly occupied $3z^2-r^2$ electrons of coppers, similar to the p_z electrons of carbons in graphene, lie from -5 to -7 eV and contributes an antiferromagnetic moment with $S=1/2$. Nonmagnetic vanadium, out of the expectation, has two electrons in V 3d orbitals. Oxygen 2p orbitals hybridizing with a small fraction of Cu 3d orbitals dominate the density of states near E_F . We also estimate that the planar nearest-neighbor and next-nearest-neighbor superexchange couplings of Cu spins are $J_1 \approx 17.5$ meV and $J_2 \approx 0.76$ meV, giving rise to a low-dimensional antiferromagnet [5]. We suggest that hole doping on O sites may bring about carriers and considerably enhance the screening, driving the system from an antiferromagnetic state to a spin liquid, or a superconducting ones, very similar to cuprates.

PACS numbers: 74.25.-q, 74.70.-b, 75.50.-y

* Corresponding author; zou@theory.issp.ac.cn

I. INTRODUCTION

Electrons in reduced dimensional lattice, for example, in two-dimensional honeycomb lattice, has less coordinate number and small spin number, they may experience strong spin fluctuations and probably form extremely low-dimensional antiferromagnet, or even exotic spin liquid state, or quantum spin Hall state, so it has attracted great interests in recent theories [1? –12]. A recent synthesized honeycomb compound $\text{In}_3\text{Cu}_2\text{VO}_9$ [14–16] is such a system with reduced dimensionality. According to the chemical valence analysis, the copper ions with $3d^9$ configuration contribute a spin-1/2 magnetic moment, while the 3d orbitals in vanadium ions are empty and contribute no magnetic moment. Due to the large separation between Cu/V-O layers, the copper spins form a quasi-two-dimensional honeycomb lattice [15]. This compound exhibits unusual magnetic behavior: it shows neither an AFM long-range order in magnetic susceptibility measurement, nor any magnetic phase transition peak in specific heat data [14, 16]. This arises great interesting whether the ground state of this compound is an example of low-dimensional antiferromagnet (AFM), or a concrete example of spin liquid system predicted by Meng *et al.* [1].

Additionally, it is well known that the electrons in graphene is a typical example of weakly interacting relativistic quantum systems. It is not very clear that how the properties of Dirac particles evolve with the increase of Coulomb interactions. Therefore the electronic motions in present transition-metal oxides $\text{In}_3\text{Cu}_2\text{VO}_9$ with the honeycomb structure is possibly a realistic testifying field of relativistic quantum mechanism for testifying how the electronic correlations or strong interaction affect the the motions and properties of the relativistic *Dirac* particles. In the mean time, the magnetic susceptibility and specific heat measurements are hard to distinguish possible ground state from a low-dimensional AFM and a spin liquid state [16]. All of these drive us to explore the electronic properties and magnetism in $\text{In}_3\text{Cu}_2\text{VO}_9$ by combining the first-principles electronic structures calculations and analytic methods, since it could provide us some first insight to this compound.

Utilizing the local density functional (LDA) and the correlation correction approaches, together with the analytical perturbation method, we show that undoped $\text{In}_3\text{Cu}_2\text{VO}_9$ is an AFM charge transfer insulator with copper $3z^2-r^2$ orbitals half filled and contributing $S=1/2$ spins. Out of our expectation, 3d orbitals in nonmagnetic vanadium have about two electrons. The oxygen 2p orbitals dominate the density of states (DOS) near E_F . We not

only extract tight-binding parameters between copper ions, but also show that $\text{In}_3\text{Cu}_2\text{VO}_9$ falls in the two-dimensional AFM regime. We also suggest the possibility that doping drives an AFM-spin liquid or superconductor transition. The rest of this paper is organized as follows: in Sec.II we briefly describe the unit cell of $\text{In}_3\text{Cu}_2\text{VO}_9$ and numerical calculation methods; in Sec.III we present the major numerical results and our analysis; Sec.IV is devoted to the conclusion.

II. NUMERICAL METHODS

We first study the electronic properties of the honeycomb compound $\text{In}_3\text{Cu}_2\text{VO}_9$ by employing the first-principles electronic structure calculation approach so as to elucidate the groundstate properties of $\text{In}_3\text{Cu}_2\text{VO}_9$. With the structural data measured by neutron powder diffraction [14], we selected 30 atoms as a magnetic unit cell $\text{In}_6\text{Cu}_4\text{V}_2\text{O}_{18}$, as seen in Fig.1. The electronic structure calculations were performed using the self-consistent full potential linearized augmented-plane-wave (FP-LAPW) scheme in the WIEN2K programme package. [17]. We used 36 k points in the irreducible part of the first Brillouin zone. The muffin-tin sphere radii were selected to be 2.36, 1.93, and 1.71 a.u. for In, Cu (V), and O in $\text{In}_3\text{Cu}_2\text{VO}_9$. The plane-wave cutoff parameter $R_{MT}K_{max}$ was 7.0, and the cutoff between the core and valence states was -6.0 Ry in all calculations. Exchange and correlation effects were taken into account in the generalized gradient approximation (GGA) by Perdew, Burk, and Ernzerhof (PBE) [18]. In order to take into account more explicitly the correlated motion of the 3d electrons of Cu (V) ions, we also performed GGA+U calculations for $\text{In}_3\text{Cu}_2\text{VO}_9$. The effective Coulomb interaction $U_{eff} = U - J_H$ (U and J_H are the on-site Coulomb interaction and the Hund's rule coupling, respectively) was used instead of U . We take $U_{eff}=8.0$ eV for copper and 4.0 eV for vanadium.

To obtain the tight-binding parameters to model the low energy process in $\text{In}_3\text{Cu}_2\text{VO}_9$ in the paramagnetic phase, we also perform the local density functional (LDA) calculations. The paramagnetic band structure calculation of $\text{In}_3\text{Cu}_2\text{VO}_9$ using the full-potential linearized augmented plane-wave plus local orbitals (FP-LAPW+lo) scheme implemented in the WIEN2K package [17]. In order to compare our numerical results with the experimental data, we adopt the experimental structural data of $\text{In}_3\text{Cu}_2\text{VO}_9$ [14]. The parent material $\text{In}_3\text{Cu}_2\text{VO}_9$ has a honeycomb layered structure with Cu atoms forming hexagonal net and

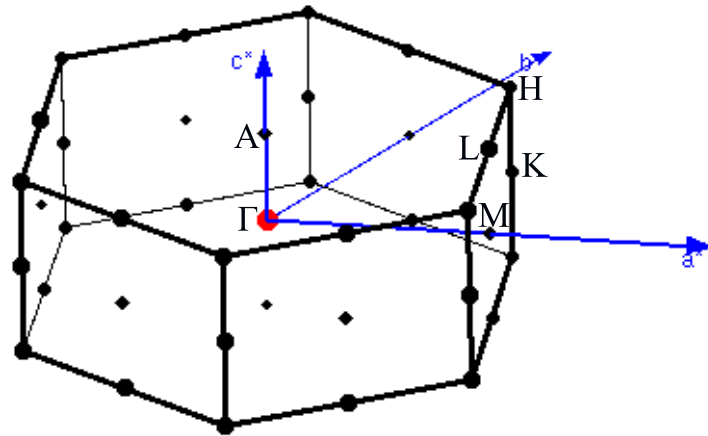
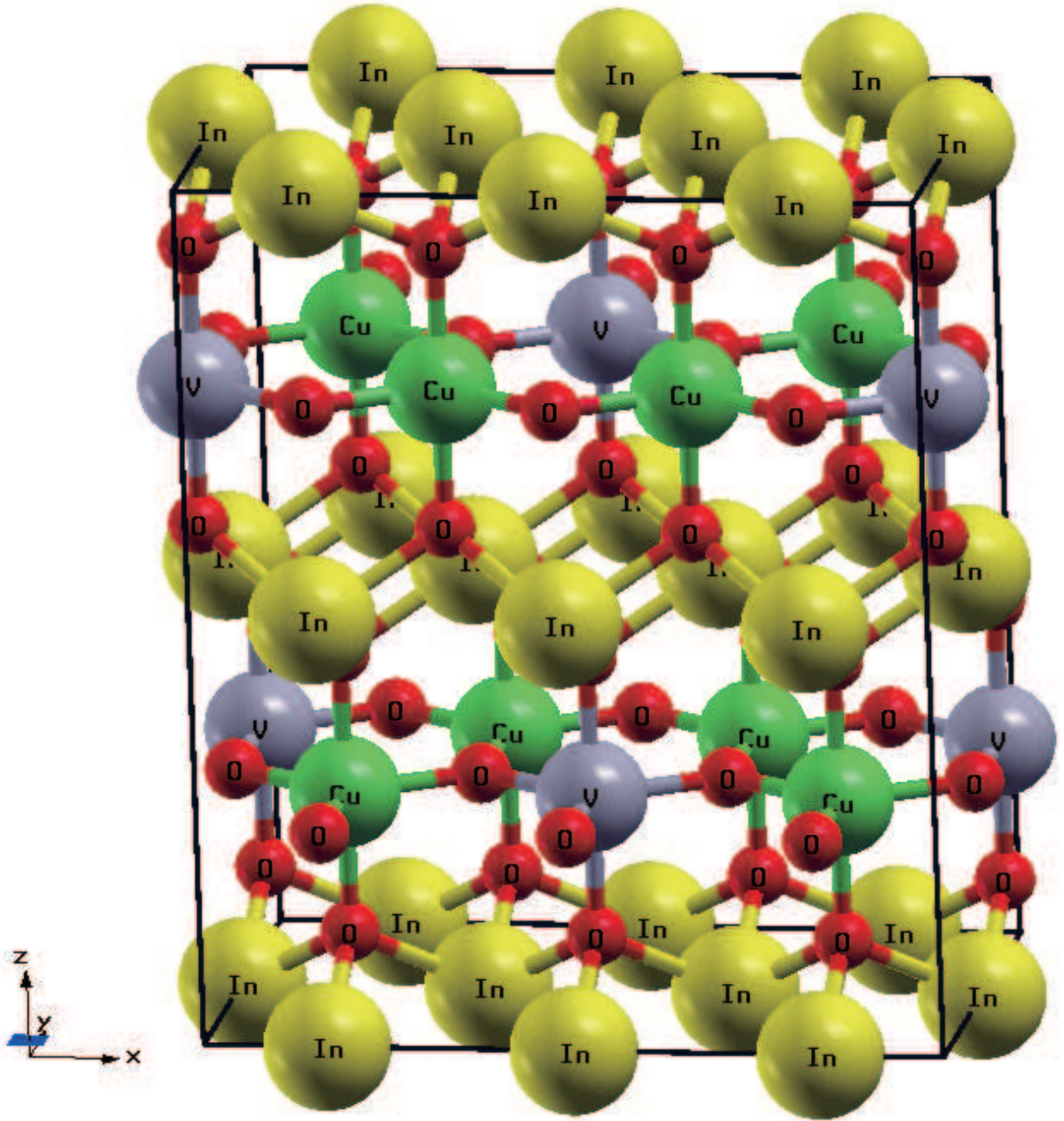


FIG. 1. (Color online) (a) Magnetic unit cell of $\text{In}_3\text{Cu}_2\text{VO}_9$, containing two crystallography primary

V atoms in the center of an hexagon. The low-temperature experimental lattice parameters are $a=3.3509\text{\AA}$ and $c=11.9012\text{\AA}$ [14]. In each unit cell there are four Cu atoms, and each Cu is coordinated by five O atoms. Detail paramagnetic band structure results are addressed in what follows.

A. Paramagnetic State

We first present the paramagnetic (*i.e.* nonmagnetic) electronic structures of $\text{In}_3\text{Cu}_2\text{VO}_9$ in Fig.2, which is obtained in the FP-LAPW scheme through the WIEN2K package. It shows that the major orbital character of the band structures near E_F is the $3z^2 - r^2$ symmetry of copper 3d orbitals. This Cu $3d_{3z^2-r^2}$ orbital in the honeycomb lattice, similar to the p_z orbital of carbon in graphene, contributes an outstanding property of the band structures in Fig.2, *i.e.* around the H point a *Dirac* cone with the approximately linear spectrum is observed. The linear energy spectrum ranges from -0.2 to 0.2 eV. We notice that the original *Dirac* point around the K points opens a small energy gap, about 0.2 eV, also as seen in Fig.2, which is attributed to the weak interlayer coupling between Cu/V-O hexagonal planes. Though the part of empty V 3d orbital are near the top of $3d_{3z^2-r^2}$ orbitals, they do not hybridize with each other. A part of filled oxygen 2p orbitals are close to the bottom of $3d_{3z^2-r^2}$ orbitals, these 2p orbitals also do not mix with $3d_{3z^2-r^2}$ orbitals, as we see in Fig.2. Thus the low-energy physics in $\text{In}_3\text{Cu}_2\text{VO}_9$ could be approximately described by the Cu $3d_{3z^2-r^2}$ orbitals across E_F .

According to the Cu $3d_{3z^2-r^2}$ orbitals mainly distributed from -1.0 eV to 0.4 eV, we extract these four Cu $3d_{3z^2-r^2}$ bands from the full band structures and fit these four bands with a single-orbital tight-bind model with the nearest-neighbor (NN), the next NN and the 3rd NN hopping integrals in the Cu/V-O plane and between the planes. These tight-binding parameters are listed in Table 1. One can easily find that the intraplane NN hopping integral t_1 is about 6 and 4 times of the intraplane NNN hopping and the interplane NN hopping, respectively, and dominates the transfer process in $\text{In}_3\text{Cu}_2\text{VO}_9$.

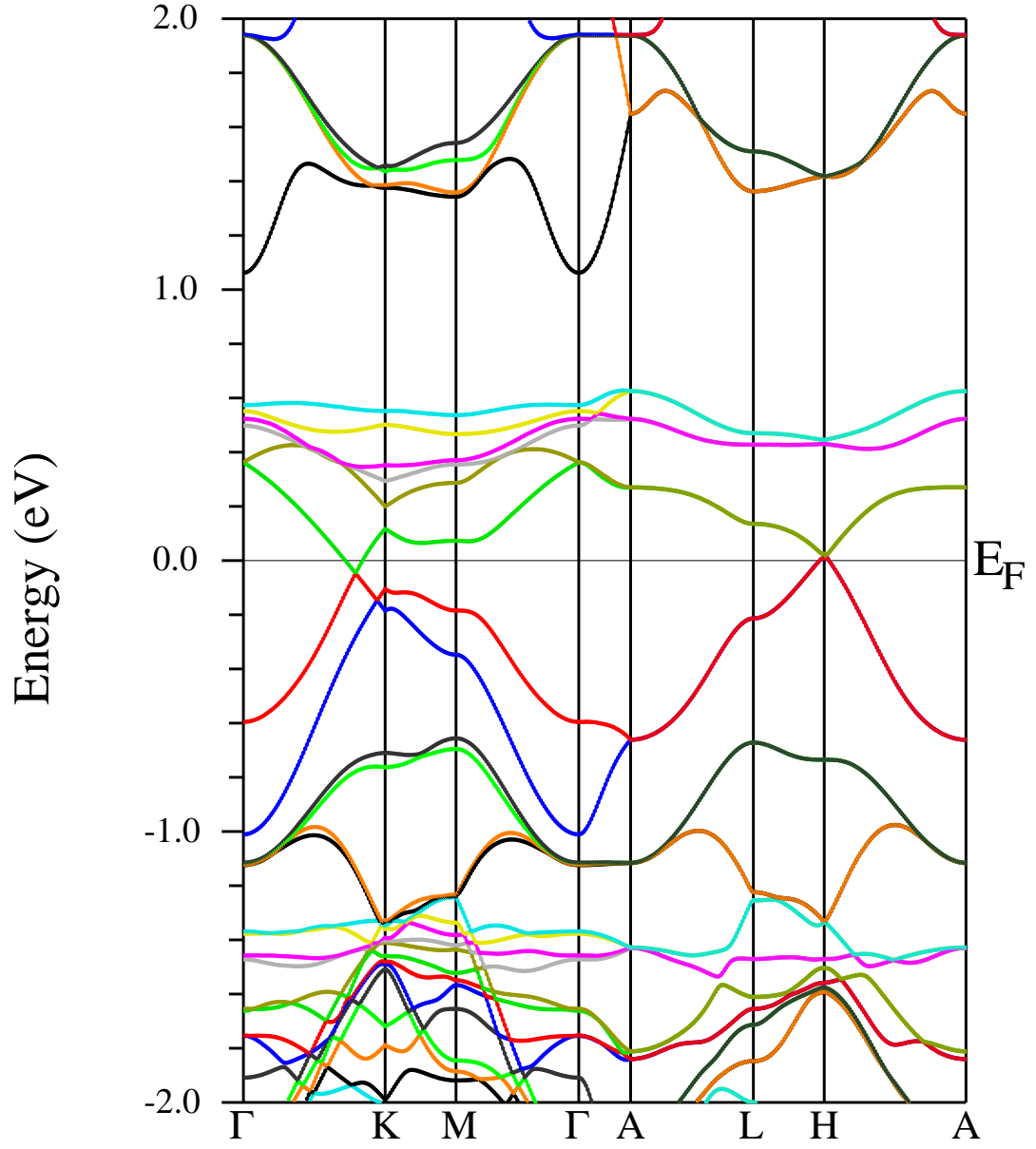


FIG. 2. (Color online) Band structures of $\text{In}_3\text{Cu}_2\text{VO}_9$ in the paramagnetic situation in the LDA framework.

B. Antiferromagnetic Ground State

To understand the insulating nature of undoped compound, we further adopt the correlation-corrected GGA (GGA+U) scheme to uncover the groundstate properties of strongly correlated $\text{In}_3\text{Cu}_2\text{VO}_9$. We consider four kinds of different magnetic configurations, nonmagnet, ferromagnet (FM), *Néel* AFM and A-type AFM, *i.e.*, interlayer AFM and intralayer FM), as the possible initial states. Our numerical results show that the total energy of the nonmagnetic state is the highest, and that of the *Néel* AFM state is the lowest. The FM and A-type AFM configurations are almost degenerate. The energy difference between the lowest *Néel* AFM and the second lowest A-type AFM or FM states is about 58.5 meV, suggesting that the magnetic coupling between Cu spins in $\text{In}_3\text{Cu}_2\text{VO}_9$ is dominantly AFM.

The system is obviously an insulator with an energy gap of 1.6 eV, as seen in Fig.3. After projecting various bands into each atom, we find that oxygen 2p orbitals consist of the major bands near E_F , ranging from 0 to -4.0 eV. While the gravity center of Cu 3d orbitals lie far from E_F . As shown in Fig.3, the center of the spin-up 3d levels lies at about -5.9 eV, and that of the spin-down 3d orbitals lies at about -4.8 eV. This gives rise to the exchange splitting of Cu 3d orbitals about $\Delta_{ex} \approx 1.1$ eV, implying that the Hund's rule coupling $J_H = \Delta_{ex}/2S \approx 1.1$ eV. Such a large exchange splitting also shows the strong Coulomb correlation on Cu 3d orbitals. Notice that the charge transfer energy between O 2p orbital and Cu 3d orbital in $\text{In}_3\text{Cu}_2\text{VO}_9$, $\Delta = \epsilon_{2p} - \epsilon_{3d}$, which is the same order to the insulating energy gap, is considerably smaller than the on-site Coulomb correlation of Cu 3d electrons, $U \sim U_{eff} = 6.0\text{-}8.0$ eV, demonstrating that undoped $\text{In}_3\text{Cu}_2\text{VO}_9$ is a charge transfer insulator.

TABLE I. Tight-binding parameters t_α and superexchange spin coupling strengths J_α in $\text{In}_3\text{Cu}_2\text{VO}_9$. Subscripts 1,2,3 and c represent the NN, next NN, 3rd NN hopping integrals or spin coupling strengths in the planes, and the NN ones between the planes, respectively. All the energies are measured in units of meV.

t_1	t_2	t_3	t_c	J_1	J_2	J_c
-180.2	-24.1	5.8	-48.9	16.2	0.3	1.2

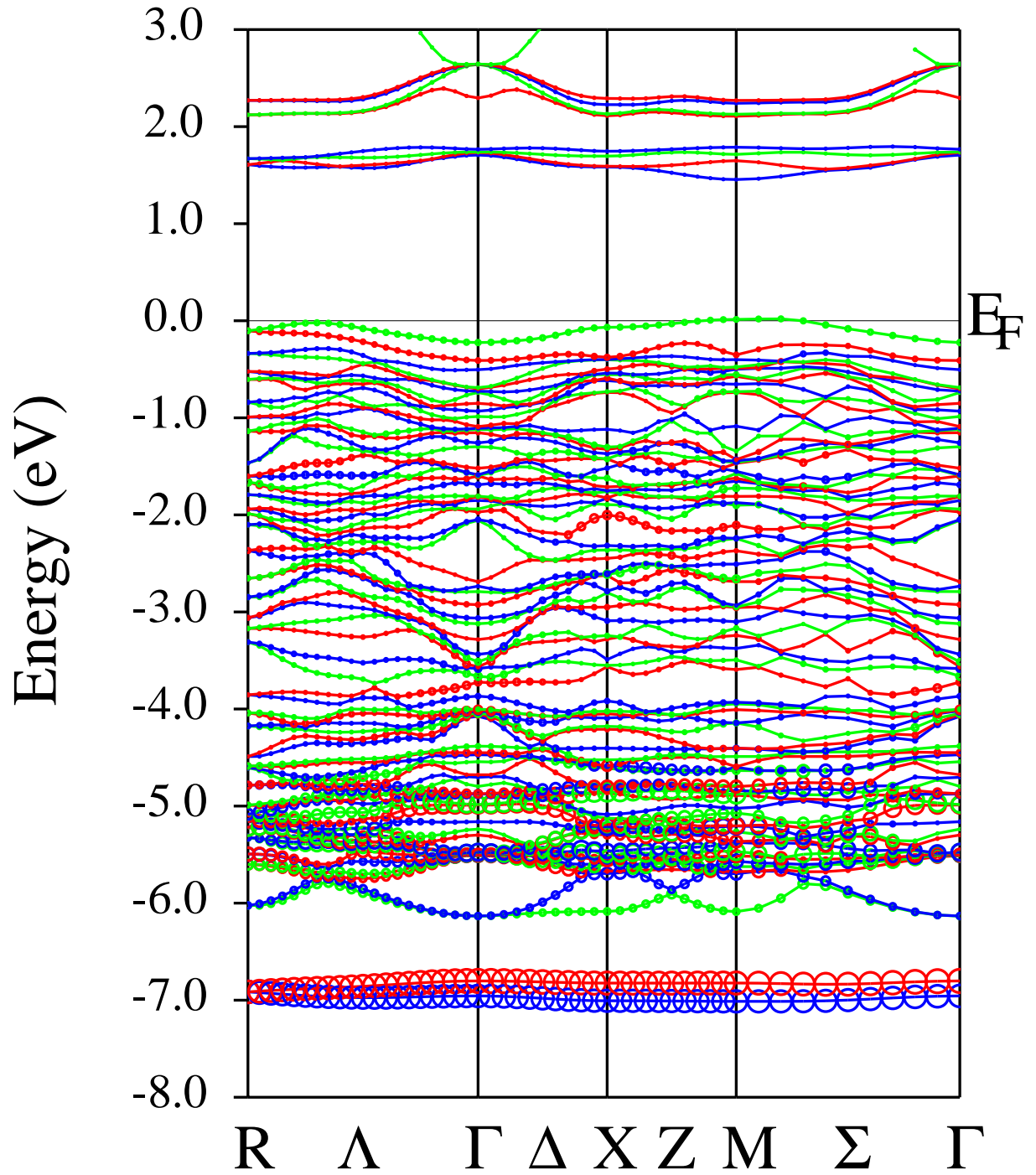


FIG. 3. (Color online) Band structures of $\text{In}_3\text{Cu}_2\text{VO}_9$ within the spin-polarized GGA+U approach. The bands marked with heavy circles are Cu 3d orbitals for spin down channel.

The charge distribution and occupation number in the 3d orbitals of Cu and V are most essential. Our results show that in the Cu 3d orbitals, the hole mainly occupies the active $d_{3z^2-r^2}$ orbital. It has a total number of 1.17 electrons, or 0.83 hole, in the $d_{3z^2-r^2}$ orbital. However, out of the early expectation and in contrary to the chemical valence analysis, V has totally 1.87 electrons in its 3d orbitals, though it shows nonmagnetic or no spin polarization in the present GGA+U ansatz. This arises from a strong $p-d$ hybridization between V and O atoms, a fraction of electrons transfer from oxygen 2p orbitals to vanadium 3d orbitals.

C. Density of States (DOS)

The density of states (DOS) projected onto each atom in Fig.4 clearly demonstrates the level distributions of Cu, V, O and In atoms. Fig.4a displays that the main DOS of copper lies from -7 eV to -4eV, though a tiny portion of 3d electrons lie between -4 eV to E_F which arises from the hybridization of Cu 3d orbital with the 2p orbitals near E_F of surrounding O or with the 3d orbitals of surrounding V atoms. One sees from Fig.4a that the $3d_{3z^2-r^2}$ orbital in Cu is almost fully spin polarized. The magnetic moment of Cu spin is contributed from the well localized spin-down $3d_{3z^2-r^2}$ orbital at the position of about 7 eV below E_F . The sharp DOS peak of Cu in Fig.4a is consistent with the spin-down flat band of Cu in Fig.3. Our orbital ground state is the $d_{3z^2-r^2}$ character, in agreement with the electron spin resonance experiment by Kataev *et al.* [19].

Meanwhile, small but finite DOS distributed from -6 eV to E_F is seen in V 3d orbitals, showing that the two 3d electrons form a wide energy band below the Fermi energy. This implies that it not only hybrids with the nearest-neighbor oxygen, but also mixes with distant Cu 3d electrons. Obviously V 3d orbitals contribute the lowest empty conduction bands in Fig.3, as we can see in Fig.4b. The projection of the DOS to each 3d orbital of V shows that the two 3d electrons in V are not spin polarized and allocates in five 3d orbitals with almost equal weight, in sharply contrast to those of Cu atoms. Fig.4c shows that In 4p orbitals give rise to a small DOS in a wide energy range. In a contrast, the DOS of oxygen is greatly larger than that of In and mainly distributes near E_F , as seen in Fig.4d. Such a strongly correlated character in $\text{In}_3\text{Cu}_2\text{VO}_9$ is very similar to that in the parent phases of high- T_c cuprates. This implies that the doping in O sites can readily affect the transport properties in $\text{In}_3\text{Cu}_2\text{VO}_9$, and easily to drive the system transit to superconducting phase

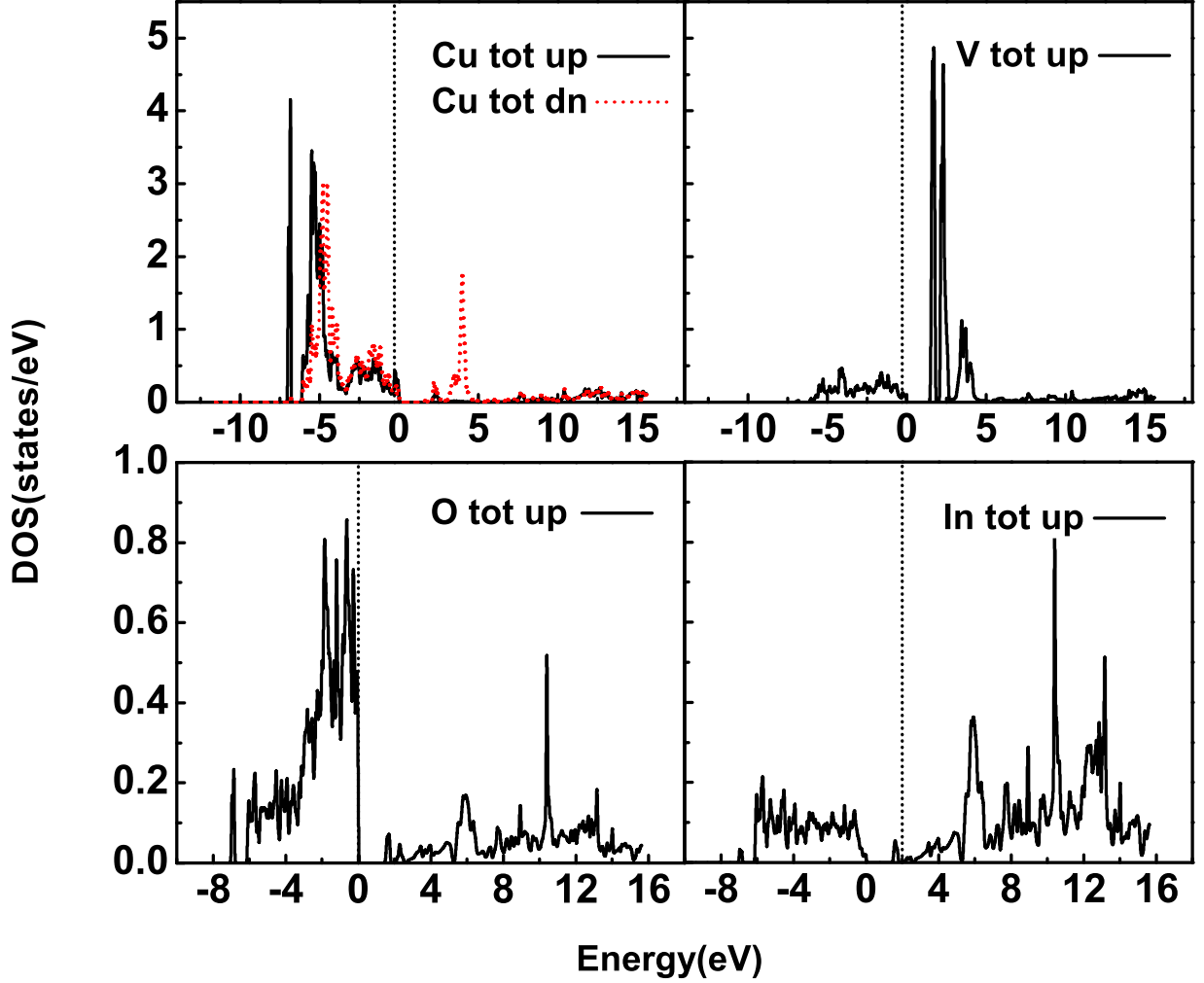


FIG. 4. (Color online) Partial density of states (DOS) of $\text{In}_3\text{Cu}_2\text{VO}_9$ within the spin-polarized GGA+U method. (a). Cu 3d orbitals; (b) V 3d orbitals; (c) In 4p orbitals, and (d) O 2p orbital at site 13.

once hole carriers are doped in oxygen 2p bands. This also suggests that doped $\text{In}_3\text{Cu}_2\text{VO}_9$ will resemble to doped cuprates in many respects.

D. Magnetism and Magnetic Couplings

The groundstate magnetic properties of $\text{In}_3\text{Cu}_2\text{VO}_9$ is the central issue of this paper. As described in the above, our numerical results demonstrate that the stablest phase is *Néel*

AFM. The magnetic moment mainly contributes from copper spins with a net total magnetic moment of $0.78 \mu_B$ per Cu atom, in which the average electron number is 0.97 in the spin-up band, and 0.19 in the spin-down one. The magnetic moment mainly arises from the $d_{3z^2-r^2}$ orbital of copper. Apparently, a strong electron correlation and a large Hund's rule coupling contribute such a large spin polarization, leading to the well defined local moment in coppers. In contrast, vanadium is nonmagnetic, though it is $3d^2$ configuration with two electrons distributing from E_F to -7.0 eV. Its nonmagnetic character may arise from the strong pd hybridization between V and O, resulting in a weak correlation in V 3d orbitals. We do not rule out the possibility of spin frustrations in the present Cu-V geometry, this may deserve further discussion in the future. Due to the full fillings of the oxygen 2p orbitals and In 4p orbitals, both O and In are not spin polarized.

The insulating nature in the undoped $\text{In}_3\text{Cu}_2\text{VO}_9$ suggests that the local spins of coppers interact through a superexchange couplings mediated via oxygens and vanadium. One expects that the possible contributions to the NN and next NN Cu-Cu superexchange couplings arise from the direct hopping between $d_{3z^2-r^2}$ electrons, the indirect hopping between Cu spins through the pd hybridization of intermediate oxygen anions, and the indirect hopping through the O-V-O bridge. To quantitatively obtain the superexchange coupling strengths, we utilize the tight-binding parameters obtained in Table I to estimate the NN and next NN superexchange couplings between Cu spins in the Cu/V-O plane and between the planes, taking the effective Coulomb interaction U as 6 eV. We obtain that the intraplane and interplane NN superexchange couplings are about $J_1 \approx 16.2$ meV and $J_c \approx 1.2$ meV, respectively, and the intraplane next NN superexchange couplings are about $J_2 \approx 0.3$ meV. More long-range spin couplings are so small to be negligible. This gives rise to $J_2/J_1 \approx 0.02$, falling in the parameter range of a two-dimensional *Néel* AFM in the J_1 - J_2 Heisenberg model [5, 22], in addition to a rather weak interlayer coupling of $J_c/J_1 \approx 0.07$, suggesting strong quasi-2-dimensionality. All of these values have been listed in Table I. Therefore, we conclude the undoped $\text{In}_3\text{Cu}_2\text{VO}_9$ is a strongly two-dimensional AFM.

We notice that the critical value between the low-dimensional AFM phase and the spin liquid one in the Hubbard model [5] is considerably smaller than that of the J_2 - J_1 Heisenberg model [22], we attribute to that the coexistence of charge and spin fluctuations expands the spin liquid or disorder region in the Hubbard model, in comparison with the Heisenberg model with only the spin fluctuation. From our analysis to the electronic state undoped

$\text{In}_3\text{Cu}_2\text{VO}_9$ can be well described by the J_2 - J_1 Heisenberg model, with the J_1 , J_2 and J_c listed in Table I.

III. REMARKS AND CONCLUSIONS

Since the experimental data of both the specific heat and magnetic susceptibility do not exhibit AFM order-paramagnet transition [16], the specific heat is almost T^2 dependent, and the magnetic susceptibility linearly increases with the lift of temperature, one naturally suspects that the ground state of undoped $\text{In}_3\text{Cu}_2\text{VO}_9$ might be a gapless spin liquid phase, a long-time searched exotic quantum phase both theoretically and experimentally, since a gapless spin liquid phase in Kagome lattice can also demonstrate similar unusual temperature-dependent behavior in the low T [3, 20]. In the mean time a strongly low-dimensional AFM may exhibit similar behaviors [21]. Our theoretical analysis based on the first-principles electronic structures calculations and band structures fitting support the latter, though it is not easily to understand why the system does not show Curie-Weiss law in the high temperature regime [16]. This exotic property is distinctly different from undoped AFM cuprates.

Moreover, as we point out above, the hole doping in O sites of $\text{In}_3\text{Cu}_2\text{VO}_9$ may introduce carriers near Fermi energy. With the increase of carriers, one expects that the screening effect can greatly reduce the Coulomb interaction, and weaken the electronic correlation. This may drive the $\text{In}_3\text{Cu}_2\text{VO}_9$ system from a *Néel* AFM ground state to a spin liquid phase [1], since in the intermediate correlation regime a half-filled Hubbard system with the honeycomb structure exist a spin-liquid ground state [1, 4]. Nevertheless, we also expect that doped $\text{In}_3\text{Cu}_2\text{VO}_9$ will not form the well-known Zhang-Rice singlet in the copper-oxygen plane of doped cuprates, since the latter arises from the hybridization between Cu $3d_{x^2-y^2}$ and O 2p orbitals, forming delocalized states in the xy plane; while in the former the $3d_{3z^2-r^2}$ orbital mixes with O 2p orbital, forming delocalized state in the z-direction. This results in completely different transport properties in doped compounds, as Yan *et al.* observed in $\text{In}_3\text{Cu}_{2-x}\text{Co}_x\text{VO}_9$ and $\text{In}_3\text{Cu}_{2-x}\text{Zn}_x\text{VO}_9$ [16].

In summary, the electronic structure and properties investigation on quasi-two-dimensional honeycomb compound $\text{In}_3\text{Cu}_2\text{VO}_9$ demonstrate that undoped phase is a charge transfer insulator with a gap of 1.6 eV, and oxygen 2p orbitals dominate the bands near E_F . Spin-1/2

local moment antiferromagnetically interacts and occupies the $3z^2-r^2$ orbital in copper. In contrast, two electrons lie in the 3d orbitals of V and are nonmagnetic. The tight-binding parameters and estimated spin coupling strengthes suggest that undoped $\text{In}_3\text{Cu}_2\text{VO}_9$ is a strongly two-dimensional *Néel* antiferromagnet. Hole doping in oxygen sites may provide the testify field of the strongly interacting *Dirac* particles, suggesting an prospective future in doped $\text{In}_3\text{Cu}_2\text{VO}_9$.

ACKNOWLEDGMENTS

We acknowledge X. H. Chen provide us original experimental data. This work was supported by the grants of the NSFC of China and of the Chinese Academy of Sciences. Numerical calculations were performed at the Center for Computational Science of CASHIPS.

-
- [1] Z. Y. Meng, T. C. Lang, S. Wessel, F. F. Assaad, and A. Muramatsu, *Nature* **464**, 847 (2010).
 - [2] S. M. Yan, D. A. Huse, and S. W. White, *Science* **332**, 1173 (2011).
 - [3] S. Saremi and P. A. Lee, *Phys. Rev. B* **75**, 165110 (2007).
 - [4] A. Vaezi and X.-G. Wen, arXiv:1010.5744; arXiv:1101.1662.
 - [5] B. K. Clark, D.A.Abanin, and S. L. Sondhi, *Phys. Rev. Lett.* **107**, 087204 (2011).
 - [6] F. Wang, *Phys. Rev. B* **82**, 024419 (2010).
 - [7] A. Liebsh, *Phy. Rev. B* **83**, 035113 (2011).
 - [8] J. He, S.-P. Kou, Y. Liang and S.-P. Feng, *Phys. Rev. B* **83** 205116 (2011); *ibid*, **84**, 035127 (2011).
 - [9] Y.-M. Lu and Y. Ran, *Phys. Rev. B* **84**, 024420 (2011).
 - [10] H. H. Zhao, Q. N. Chen, Z. C. Cai, M. P. Qin, G. M. Zhang, and T. Xiang, arXiv:1105.2716.
 - [11] W.-S. Wang, Y.-Y. Xiang, Q.-H. Wang, F. Wang, F. Yang, and D.-H. Lee, *Phys. Rev. B* **85**, 035412 (2012).
 - [12] W. Wu, S. Rachel, W.-M. Liu, and K. Le Hur, arXiv:1106.0943.
 - [13] T. Li, *Euro. Phys. Lett.* **97**, 37001 (2012).

- [14] A. Möller, U. Löw, T. Taetz, M. Kriener, G. Andre, F. Damay, O. Heyer, M. Braden, and J. A. Mydosh, Phys. Rev. B **78**, 024420 (2008).
- [15] M. Yehia, E. Vavilova, A. Moeller, T. Taetz, U. Loew, R. Klingeler, V. Kataev, and B. Buechner, Phys. Rev. **B 81**, 060414(R) (2010).
- [16] Y.-J. Yan, Z.-Y. Li, T. Zhang, X.-G. Luo, G.-J. Ye, Z.-J. Xiang, P. Cheng, L.-J. Zou, and X. H. Chen, arXiv:1106.1713, accepted to Phys. Rev. B (2012).
- [17] P. Blaha, K. Schwarz, G. Madsen, D. Kvasnicka, and J. Luitz: "Computer Code WIEN2k, an augmented plane wave plus local orbitals program for calculating crystal properties", Karlheinz Schwarz, Technische Universität Wien, Austria, (2001).
- [18] J. P. Perdew, K. Burk, and M. Ernzerhof, Phys. Rev. Lett. **77**, 3865 (1996).
- [19] V. Kataev, A. Möller, U. Löw, W. Jung, N. Schittner, M. Kriener, and A. Freimuth, J. Magn. Magn. Mater. **290-291**, 310 (2005).
- [20] Y. Ran, M. Hermele, P. A. Lee, X.-G. Wen, Phys. Rev. Lett. **98**, 117205 (2007).
- [21] K. Oka, I. Yamada, M. Azuma, S. Takeshita, K. H. Satoh, A. Koda, R. Kadono, M. Takano, and Y. Shlmakawa, Inorg. Chem, **47**, 7355 (2008).
- [22] F. Mezzacapo and M. Boninsegni, Phys. Rev, **85**, 060402 (2012).